ARTICLE

Journal of Materials Chemistry
www.rsc.org/materials

Functional glass slides for *in vitro* evaluation of interactions between osteosarcoma TE85 cells and mineral-binding ligands

Jie Song,*[a,b] Julia Chen,[a] Catherine M. Klapperich,[c] Vincent Eng[a] and Carolyn R. Bertozzi*[a,b,d]

[a] *Materials Sciences Division, Lawrence Berkeley National Laboratory, University of California, Berkeley, California 94720, USA. E-mail: JSong@lbl.gov; Fax: 1 510 486 4995; Tel: 1 510 486 4125*
[b] *The Molecular Foundry, Lawrence Berkeley National Laboratory, University of California, Berkeley, California 94720, USA*
[c] *Departments of Manufacturing and Biomedical Engineering, Boston University, Massachusetts 02215, USA*
[d] *Departments of Chemistry and Molecular and Cell Biology, and Howard Hughes Medical Institute, University of California, Berkeley, California 94720, USA. E-mail: crb@berkeley.edu; Fax: 1 510 643 2628; Tel: 1 510 643 1682*

Received 5th March 2004, Accepted 20th July 2004
First published as an Advance Article on the web 5th August 2004

Primary amine-functionalized glass slides obtained through a multi-step plasma treatment were conjugated with anionic amino acids that are frequently found as mineral binding elements in acidic extracellular matrix components of natural bone. The modified glass surfaces were characterized by X-ray photoelectron spectroscopy (XPS) and contact angle measurements. Human osteosarcoma TE85 cells were cultured on these functionalized slides and analyses on both protein and gene expression levels were performed to probe the "biocompatibility" of the surface ligands. Cell attachment and proliferation on anionic surfaces were either better than or comparable to those of cells cultured on tissue culture polystyrene (TCPS). The modified glass surfaces promoted the expression of osteocalcin, alkaline phosphatase activity and ECM proteins such as fibronectin and vitronectin under differentiation culture conditions. Transcript analysis using gene chip microarrays confirmed that culturing TE85 cells on anionic surfaces did not activate apoptotic pathways. Collectively, these results suggest that the potential mineral-binding anionic ligands examined here do not exert significant adverse effects on the expression of important osteogenic markers of TE85 cells. This work paves the way for the incorporation of these ligands into 3-dimensional artificial bone-like scaffolds.

Introduction

In recent years, steady progress has been made in constructing functional tissue engineering (TE) scaffolds for tissue replacement.[1–3] In addition to the chemical, physical and mechanical integrity of the material,[4–6] focus has been directed toward assessment of the biocompatibility of these artificial TE scaffolds.[7] When exposed to a cellular environment, an acceptable TE scaffold should not trigger an apoptotic (programmed cell death) pathway. Ideally, the material will instead assist the site of implant to resume its normal function. For instance, an ideal artificial bone implant should not only withstand the necessary mechanical loading, but also promote the synthesis and secretion of extracellular matrix (ECM) proteins of surrounding/invading bone cells and facilitate the nucleation and growth of biominerals.

The evaluation of cell–material interactions, however, is far from straightforward. One difficulty associated with interpreting the interactions of cells with a 3-D synthetic material is that it is hard to separate out the influence of chemical modifications from various physical factors, such as surface roughness, porosity and the pore size of the scaffold. Therefore, a general strategy for isolating one contributing factor at a time, such as the role chemical modifications play in cell–material interactions, is desired.

Here we propose the use of 2-D functional surfaces to assist the evaluation of specific interactions between cells and functional ligands, an important step in an iterative material design approach toward a biocompatible 3-D functional scaffold (Fig. 1). Specifically, we propose to display ligands intended for 3-D TE scaffolds on 2-D model surfaces *via* convenient surface modifications. *In vitro* analyses performed with cells cultured

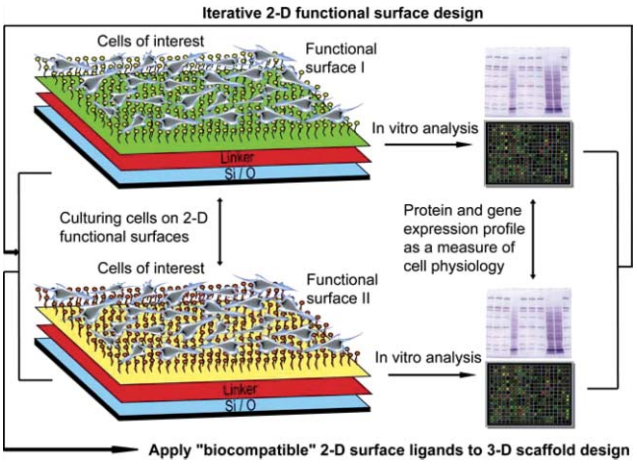

Fig. 1 A 2-D functional surface-based strategy to probe cell–ligand interactions: an iterative design approach toward biocompatible 3-D tissue engineering (TE) scaffold. Chemical ligands intended for 3-D TE scaffolds are covalently attached to 2-D glass surfaces *via* appropriate linkers. *In vitro* analyses performed with cells cultured on these functional surfaces will be used as a measure of cellular responses to specific chemical modifications. Only non-cytotoxic ligands will be further used for 3-D scaffold construction. Ligands exerting adverse effects on cells of interest will be either rejected or modified to improve their biocompatibility.

DOI: 10.1039/b408597n

on these functional surfaces can then be used as a measure of cellular responses to specific chemical modifications. Functional ligands will be either rejected, modified for improvements, or established as biocompatible and enter the next phase of 3-D scaffold construction.

To realize this strategy, we developed a surface functionalization approach based on plasma treatment that introduces reactive primary amine functionalities and subsequent straightforward bioconjugation chemistry that attaches various ligands of interest. Although primary amines can be introduced by reacting glass surfaces with aminosilane derivatives,[8–11] we favor the plasma treatment approach as it can be applied to a wide range of substrates including glass, metals, ceramics and polymers without significant modifications to the experimental protocol. In this case study, the effects of osteosarcoma cell interactions with mineral binding ligands on both protein and gene expression levels were probed.

Experimental

Surface functionalization

A multi-step plasma treatment (hydrocarbon treatment followed by allylamine treatment) on plain microscope glass slides (3 in × 1 in, Corning, NY, USA), performed at 4th State, Inc. (Belmont, CA, USA), yielded primary amine-functionalized slides. The plasma-treated slides were then immersed in a 25% (v/v) glutaraldehyde aqueous solution placed over an orbital shaker at rt for 16 h. After removing excess glutaraldehyde and rinsing with Millipore water, the aldehyde-functionalized slides were then placed in 40 mg mL^{-1} L-aspartic acid (L-Asp), L-glutamic acid (L-Glu), L-serine (L-Ser), glycine (Gly), L-phosphoserine (L-Ser*) and tetrapeptide Gly-Asp-Ser*-Ser* solutions (solubilized by the addition of KOH, pH 7–8), respectively. The coupling *via* Schiff base formation was allowed to proceed at rt for 16 h over an orbital shaker. The procedure is depicted in Fig. 2. After being rinsed with Millipore water and air-dried, the functionalized slides were stored in a dessicator until further analysis or used directly for cell culture experiments.

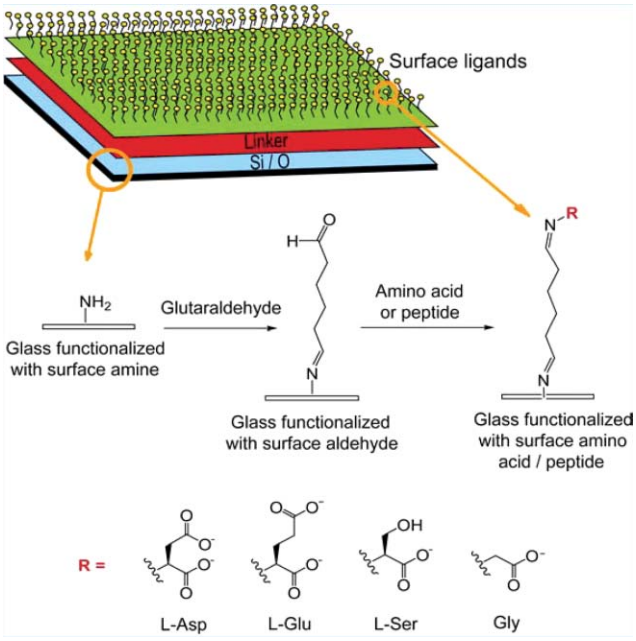

Fig. 2 Functionalization of 2-D glass surfaces with anionic ligands. Primary amine-terminated glass slides obtained through a multi-step plasma treatment can be further coupled with the N-termini of amino acids or peptides of interest *via* a glutaraldehyde linker. In this study, L-Asp, L-Glu, L-Ser and Gly were covalently attached to the surface *via* Schiff base linkers, exposing anionic surface carboxylates.

Surface elemental analysis of functionalized surfaces

The covalent coupling of glutaraldehyde and amino acids to the glass surfaces was confirmed by X-ray photoelectron sprectroscopy (XPS) analysis performed on a PHI 5400 ESCA/XPS instrument. All surface elemental analyses were performed at a 45° takeoff-angle with a 400 W Al anode X-ray source. An average from analyses performed over three randomly selected areas for each functional surface was reported.

Contact angle measurements

The wettability of each functionalized surface was characterized by contact angle measurements. The static contact angles were measured with a goiniometer within 10 s after depositing a water droplet on the surface of interest. At least three droplets of water were placed over each surface type and the angles were reported as an average of all measurements.

Cell culture

Human osteosarcoma TE85 cells were seeded onto six types of glass slides (L-Asp, L-Glu, L-Ser, Gly and NH_2 functionalized slides as well as plain glass slides, 5 slides for each surface type) and tissue culture polystyrene (TCPS) control at an initial density of 5000 cells cm^{-2}. Cells were cultured at 37 °C in a humidified incubator with 5% CO_2 in Osteoblast Growth Media (OGM, Clonetics Walkersville, MD, USA) supplemented with L-ascorbic acid[12] and Clonetics OGM Differentiation SingleQuots (containing β-glycerolphosphate and hydrocortisone)[13] and 1 nM dihydroxyvitamin D3.[14]

Fluorescence labelling of aldehyde-modified surfaces

Aldehyde-functionalized slides were reacted with Texas Red hydrazide (0.3 mM, Molecular Probes, Eugene, OR, USA) in 2-[*N*-morpholino]ethanesulfonic acid (MES) buffer (0.1 M, pH 6.1) with or without 3 mM $NaBH_3CN$[15] at rt overnight. Plain glass slides were exposed to Texas Red hydrazide under the same condition to account for non-specific adsorption of the fluorescent dye. After thoroughly rinsing with water to remove excess dye, these slides were incubated under cell culture conditions in Osteoblast Growth Media supplemented with differentiation factors described above for 6 and 32 h. Images of the slides before and after incubation with cell culture media were acquired on an Olympus BX51 fluorescent microscope equipped with a digital camera. The same magnification and exposure time were applied for all slides. The mean fluorescence intensity of each image was calculated by an image processing software ImageJ.

Optical microscopy

Optical microscopy images of TE85 cells attached on functionalized surfaces, plain glass and TCPS control at 6 and 32 h after initial cell seeding were acquired with an inverted light microscope (Nikon Eclipse TS100) equipped with a digital camera. Cell attachment and spreading on each surface were examined.

Cell lysate collection

After 6 and 32 h of culture, TE85 cells attached to functionalized slides and TCPS control were lysed in RIPA buffer (50 mM Tris–HCl, pH 7.4, 150 mM NaCl, 1% Triton X-100, 0.1% SDS, 0.5% sodium deoxycholate, 0.02% sodium azide) in the presence of protease inhibitors. Crude lysates were shaken at 4 °C for 30 min before they were centrifuged and supernatants collected. Lysates collected from 3 and 2 slides of each surface type were pooled for the 6 and 32 h isolation, respectively.

Total protein content determination

The total protein content of cell lysates was determined using a BCA Protein Assay Reagent Kit (Pierce, Rockford, IL, USA).

Quantitative DNA assay

The DNA content of cell lysates collected from various surfaces at 6 and 32 h was determined using a PicoGreen dsDNA quantification kit (Molecular Probes, Eugene, OR, USA).

Alkaline phosphatase (ALP) assay

ALP activity was determined by a fluorescence assay (Alkaline Phosphatase Reporter Gene Detection Kit, Sigma, St. Louis, MO, USA). The assay was performed on culture media collected 6 and 32 h after initial cell seeding. The fluorescence intensity was recorded on a Spectra Max Gemini XS fluorescence plate reader (Molecular Devices, Sunnyvale, CA, USA).

Detection of osteocalcin

Osteocalcin (OC) secreted to the culture media was quantitized using microtiter plate immunoassay (Mid-Tact Human Osteocalcin EIA Kit, BTI, Stoughton, MA, USA).[16,17] The concentrations of osteocalcin secreted in media by TE85 cells cultured on all surface types and at time points of 6 and 32 h were determined following the manufacturer's protocol.

Western blots

Cell lysates collected from various surfaces at 6 h (4.5 μg per lane) were separated on Criterion XT pre-cast gels (10% Bis-Tris, Bio-Rad Laboratories, Hercules, CA, USA), and electrotransferred to nitrocellulose membranes (VWR Scientific Products, Brisbane, CA, USA). After blocking with 5% non-fat milk, the membranes were incubated with mouse monoclonal fibronectin IgG (1 : 1000, Sigma Chemical, St. Louis, MO, USA), mouse monoclonal vitronectin IgG (1 : 1000, Sigma Chemical, St. Louis, MO, USA) and mouse monoclonal α-tubulin IgG (1 : 5000, Santa Cruz Biotechnology, Santa Cruz, CA, USA) for 1 h at rt, respectively. Visualization was performed with a horseradish peroxidase (HRP)-conjugated secondary antibody, goat anti-mouse IgG-HRP (1 : 5000, incubated for 1 h at rt, Santa Cruz Biotechnology, Santa Cruz, CA, USA) and the ECL™ Advance Western Blotting Detection Kit (Amersham Biosciences, Piscataway, NJ, USA). The blots were imaged with a ChemiDoc XRS Photodocumentation System (Bio-Rad Laboratories, Hercules, CA, USA).

RNA isolation and microarray chip hybridization

In a parallel experiment, TE85 cells were cultured in Dulbecco's Modified Eagle's Medium (DMEM, Gibco, Carlsbad, CA, USA) supplemented with 10% FBS, 100 U mL^{-1} penicillin and 100 mg L^{-1} streptomycin on various anionic surfaces and TCPS. Total RNA was isolated at time points of 6 and 32 h using Qiagen RNeasy Kits (Qiagen, Valencia, CA, USA). The RNA isolated from each sample was quantified by the absorption at 260 and 280 nm, and characterized by denaturing agarose gel electrophoresis (data not shown). Non-degraded RNA samples were then reverse transcribed, amplified, labelled, hybridized to Affymetrix U133A Human GeneChips, and scanned at the Microarray Resource Center at Boston University.

Statistical analyses

Each gene on the chip is represented by several unique oligonucleotides (a probeset) and is used to quantify the level of a gene transcript present in the sample. To determine which transcript levels changed significantly between the different surfaces, robust multi-chip analysis (RMA)[18,19] that minimizes the likelihood of false positives was performed. The single expression values generated using RMA for each probeset (gene) was summarized and sorted by probeset. For each probeset there were 10 data points corresponding to different time (6 and 32 hours) and surface conditions.

A two-way ANOVA analysis was then performed for each of the 22,283 probesets with respect to time and surface treatment and the interaction term of time and surface treatment using a model generated with Stata (Stata Corporation, College Station, TX).[7] Genes (probesets) with significant p values ($p < 0.001$) were considered differentially expressed.

Results and discussion

Amine-functionalized glass slides were obtained *via* plasma treatment. Unlike ammonia plasma treatment,[20] the allyl amine plasma treatment used here preferentially introduced primary amines over secondary amines on the surface of hydrocarbon-coated glass slides,[21–23] exposing maximum reactive sites for further functionalization. XPS analysis (Table 1) showed that the plasma-treated glass surface was fairly well covered by hydrocarbons and amines, exposing a negligible amount of Si (Si/C ~ 0.03) from the underlying glass substrate.

As shown in Fig. 2, upon exposing the amine functionalized-slides to glutaraldehyde, reactive surface aldehydes were installed which were then readily coupled with ligands of interest. We attached a number of amino acids and peptides including L-Glu, L-Asp, L-Ser, Gly, L-Ser* and Gly-Asp-Ser*-Ser* to the slide surface *via* Schiff base formation. These surface ligands vary in both the number and the type of anionic residues. Anionic amino acids L-Glu, L-Asp and L-Ser* as well as hydroxy amino acid L-Ser have been identified as abundant residues in acidic mineral nucleating ECM proteins of various calcified tissues.[24–28] Although their roles in controlling the nucleation, growth and stabilization of transitional phases of biominerals in calcified tissues are still under debate, the incorporation of these ligands in artifical bone-like scaffolds to

Table 1 Average O/C, N/C and Si/C ratios from XPS surface elemental analysis and water contact angles of plasma-treated glass slides and amino acid-functionalized slides

	XPS analysis[a]			
Functional surfaces	N/C	O/C	Si/C	Static contact angle/°[b]
NH_2	0.5288 ± 0.0263	0.3038 ± 0.0176	0.0327 ± 0.0049	54.0 ± 0.5
Glutaraldehyde	0.2610 ± 0.0274	0.8938 ± 0.0852	0.0508 ± 0.0074	50.5 ± 2.0
L-Asp	0.3383 ± 0.0142	0.9323 ± 0.0987	0.0802 ± 0.0142	37.0 ± 0.5
L-Glu	0.2638 ± 0.0131	0.7915 ± 0.0597	0.0729 ± 0.0068	37.5 ± 1.0
L-Ser	0.3237 ± 0.0162	0.8170 ± 0.0723	0.0580 ± 0.0081	48.5 ± 1.0
Gly	0.3212 ± 0.0130	0.5109 ± 0.0108	0.0487 ± 0.0097	41.5 ± 1.5

[a] Photoelectron lines used in XPS analysis: C, 1s; O, 1s; N, 1s; Si, 2p3. [b] The static contact angles were measured within ten seconds after depositing a water droplet on the surface of interest.

stimulate mineral integration is an intriguing idea. The straightforward surface modification presented here serves as a convenient way to present potential mineral-binding ligands for the investigation of their interaction with both biominerals and bone cells.

All functionalized surfaces including the intermediate aldehyde-functionalized surface were characterized by XPS and contact angle measurements. XPS analysis showed relative changes of N/C and O/C ratios consistent with the respective surface derivatizations (Table 1). For instance, a drop in N/C ratio and an increase in O/C ratio is expected when the surface is modified from NH_2-terminated to aldehyde-terminated. It is also expected that Asp-terminated surface should show a higher O/C ratio and a comparable N/C ratio than the Gly-terminated surface since the former contains 1N and 4 O's per surface residue while the latter contains 1 N and 2 O's per surface residue. These were indeed what we observed experimentally. We also observed a slight increase in Si levels after each ligand attachment (Table 1). The exposure of a small amount of Si–O glass surface is likely to arise from mechanical abrasion during the functionalization and the subsequent extensive rinsing process. Dectection of P on phosphorylated surfaces has not been consistent (data not shown), likely due to varying degrees of β-elimination of the phosphate groups occurring during Schiff base formation under slightly basic conditions. Suffering from low reproducibility, the phosphorylated surfaces (Ser* and Gly-Asp-Ser*-Ser*) were therefore excluded from further *in vitro* evaluations.

The wettability of each functionalized surface was determined by contact angle measurement. A lower water contact angle indicates a more hydrophilic and polar material surface. As expected, the contact angles of the anionic surfaces were lower than both the primary amine-functionalized control slide and the aldehyde-functionalized slide (Table 1). Among all, L-aspartate and L-glutamate-modified surfaces gave the smallest contact angles, reflecting the most polar charactistics (two carboxylates per site of modification) of all surfaces examined. It is interesting to note that the L-Ser-functionalized surface gave rise to a much higher contact angle than the Gly-functionalized surface. Intermolecular H-bonding between the carboxylate and hydroxyl groups exposed at the L-Ser surface may have contributed to the lowering of its overall hydrophilicity.

To probe the chemical stability of Schiff base linkage (N=C) in aqueous cell culture conditions, a fluorescence labelling study was conducted. Texas Red hydrazide was covalently conjugated to the aldehyde-terminated glass slides under non-reductive and reductive conditions, yielding fluorescently-labelled surfaces containing N=C and the more stable N–C linkages, respectively. As shown in Fig. 3, after 6 and 32 h incubation with cell culture media, slides labelled under both conditions maintained their fluorescence intensity at comparable levels. This suggests that the Schiff base linkage is stable under cell culture condition for at least 32 h, and is therefore suitable for the current investigation. However, for experiments that will involve longer incubations of functional slides in aqueous media where hydrolysis of the Schiff base could pose a serious problem, formation of the more stable N–C bond *via* reductive amination may be considered as a practical alternative.

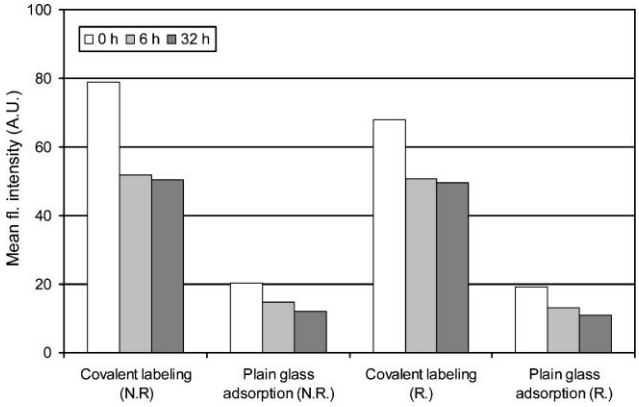

Fig. 3 Relative stability of C=N *vs.* C–N linkage under cell culture conditions as determined by fluorescence labelling. Texas Red hydrazide was covalently attached to the aldehyde surface *via* C=N and C–N linkages under non-reductive (N.R.) and reductive (R.) conditions, respectively. Plain glass slides were also treated with the dye for same periods of time to account for non-specific adsorption. Fluorescently-labelled slides were incubated with OGM differentiation media at 37 °C for 6 and 32 h before analysis by fluorescence microscopy. The mean fluorescence intensity of each image was computed by ImageJ software.

To determine whether the anionic surfaces exert intrinsically adverse effects on the proliferation and osteogenic potential of bone cells, we exposed these functionalized slides to osteosarcoma TE85, a human bone tumor cell line, at a constant seeding density and under identical culture conditions. Human osteosarcoma TE85 cells are easy to culture and are known to express osteoblastic phenotypes.[29–31] They have been widely used as experimental models for investigating osteoblast functions.[32–38] Optical images acquired at 6 h after initial seeding (Fig. 4) showed that TE85 cells attached to and spread over all surfaces examined. Cells attached to anionic and primary amine surfaces adopted well-spread morphologies that were comparable to those observed on TCPS. In contrast, fewer

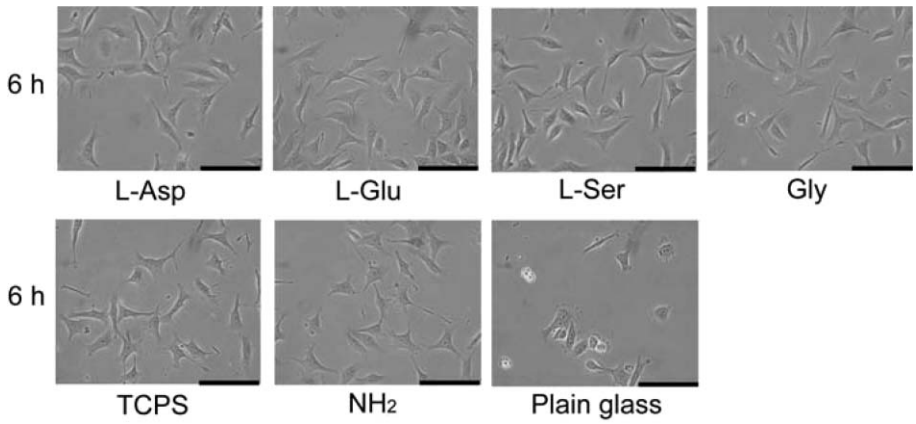

Fig. 4 TE85 cell attachment and spreading on anionic functional surfaces, TCPS, NH_2-functionalized surface and plain glass control at 6 h after initial seeding. Scale bars are 100 μm. Note that TE85 cells attached and spread on anionic surfaces and the primary amine surface with morphologies similar to those observed when attached to TCPS. In contrast, fewer cells were attached to the plain glass surface at 6 h after initial seeding, with more rounded morphologies.

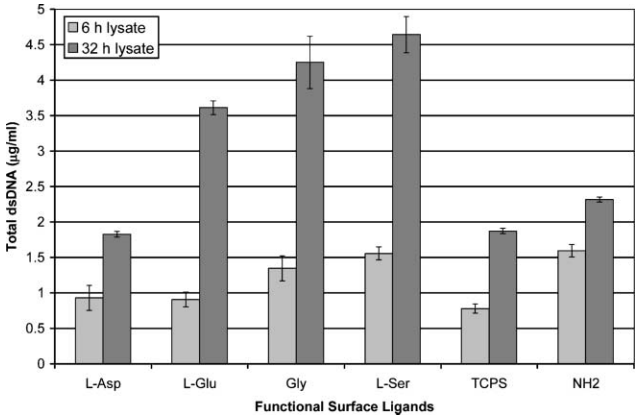

Fig. 5 Quantification of dsDNA in cell lysates collected from different functional surfaces at 6 and 32 h after initial cell seeding. Error bars indicate the standard deviation of the mean for three replicate experiments.

TE85 cells attached to the plain glass surface at 6 h after initial seeding, and these cells showed a more rounded morphology. This result is expected as it is known that untreated microscope glass slides are not suitable substrates for cell attachment. These plain glass slides were therefore excluded from further assays. TE85 cells attached to anionic surfaces proliferated at a comparable or higher rate than those attached to TCPS. By 32 h, a near-confluent cell layer was formed on every anionic surface (image not shown). Cell proliferation was also evidenced by quantitative DNA assays performed on cell lysates collected from various surfaces at 6 and 32 h, as shown in Fig. 5. This result confirms that anionic surfaces were superior substrates for attachment and proliferation of TE85 cells compared to TCPS.

ALP activity is a marker of early osteoblastic differentiation.[39] We compared the alkaline phosphatase activity detected in the cell culture media at both time points to probe the effect of anionic surface ligands on normal differentiation of bone cells. Normalized ALP activity was plotted as a function of culture time and surface ligands. As shown in Fig. 6, TE85 cells cultured on the tested anionic surfaces secreted more alkaline phosphatase into the culture media over a period of 32 h than at 6 h, while no significant increase of ALP activity after 6 h was detected with cells cultured on TCPS or amine functionalized glass surfaces.

We also monitored the expression of osteocalcin, a major non-collagenous protein of bone and a marker of osteoblast maturation.[14,39] While the precise biological function of osteocalcin is not known, it is the most specific marker of

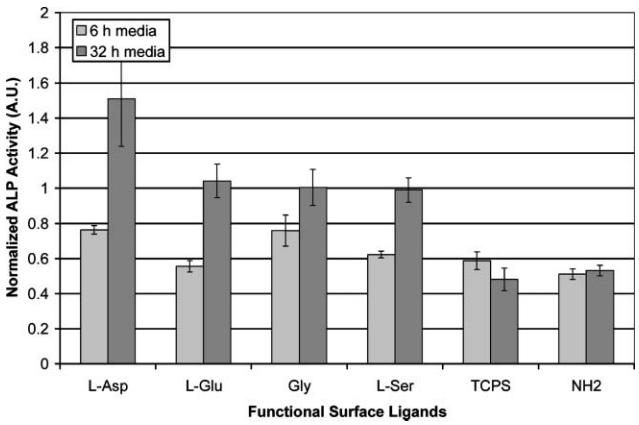

Fig. 6 Normalized alkaline phosphatase (ALP) activity in culture media as a function of culture time and surface ligands. Error bars indicate the standard deviation of the mean for three replicate experiments.

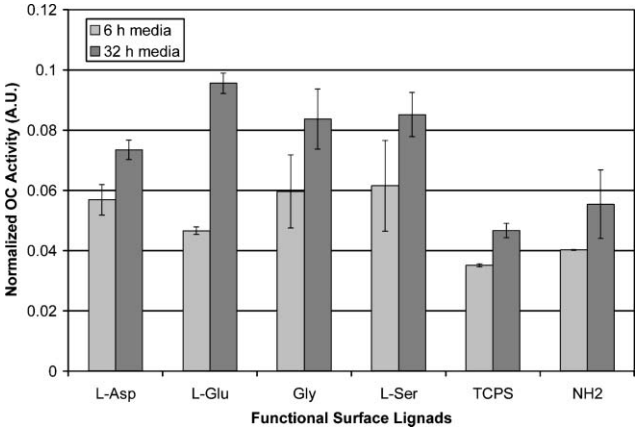

Fig. 7 Normalized osteocalcin (OC) activity in media as a function of culture time and surface ligands. Error bars indicate the standard deviation of the mean for three replicate experiments.

osteoblastic function described to date.[40] Although the majority of osteocalcin is deposited into the extracellular matrix of bone, a small fraction of it is secreted directly into the circulation *in vivo*. We compared the amount of osteocalcin secreted in media by TE85 cells cultured on various surfaces in the presence of 1,25-dihydroxyvitamin D3, a differentiation factor known to stimulate osteocalcin production when supplemented for a short duration in culture.[14] Normalized OC activity was plotted as a function of culture time and surface ligands. As shown in Fig. 7, TE85 cells showed varied degrees of sustained osteocalcin seretion in culture media during proliferation on different surfaces, with higher levels of ALP detected in cultures performed on anionic surfaces.

The expression of the ECM proteins vitronectin and fibronectin, as well as the cytoskeletal protein α-tubulin by TE85 cultured on anionic surfaces and TCPS control at 6 h was monitored by Western blot (Fig. 8). We observed a slightly lower expression of α-tubulin in TE85 cells cultured on anionic surfaces, whereas the expression of vitronectin and fibronectin seem to be stimulated by culture on the anionic surfaces. Taken together, our *in vitro* analysis results suggest a favorable interaction between TE85 cells and wholly synthetic mineral binding anionic motifs, suggesting an osteophilic nature of these ligands. It is tempting to draw a parallel between this observation and the critical role anionic non-collagenous ECM proteins play in bone formation and remodelling in nature.

Finally, we compared the gene expression profiles of TE85 cultured in expansion media on the anionic surfaces *vs.* TCPS. Oligonucleotide microarrays (U133A Human GeneChip, Affymetrix, Santa Clara, CA) were employed to quantify transcript levels at 6 and 32 h time points as the cells attached and proliferated on the functionalized surfaces. Statistical analysis ($p < 0.001$) identified a relatively small set of differentially expressed genes for each anionic surface relative to TCPS from over 22,200 well-substantiated human genes. Among them, no genes directly related to the activation of apoptotic pathways were identified. This is consistent with the minimal

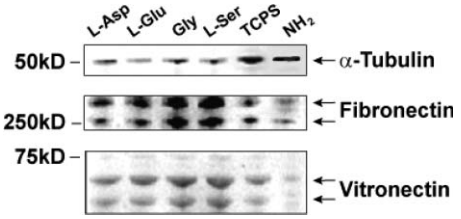

Fig. 8 Expression of α-tubulin, fibronectin (FN), and vitronectin (VN) by TE85 cells cultured on different functional surfaces at 6 h (4.5 μg lysate per lane) after initial cell seeding.

cytotoxicity of these anionic ligands observed in cell culture experiments. We also did not observe differential expression of genes encoding osteogenic markers such as osteocalcin and alkaline phosphatase, which may be attributed to the non-differntiating culture condition used for the microarray study. The complete gene expression data are available in the NCBI Gene Expression Omnibus database (http://www.ncbi.nlm.nih.gov/geo/)[41] under accession numbers GSM15785–GMS15795.

Conclusion

We have developed a straightforward surface modification method for investigating the effects of functional ligands on cellular processes. These data will be useful in the design and evaluation of the biocompatibility of 3-D tissue engineering scaffolds. The presentation of functional ligands on a 2-D surface reduces the number of interfering factors to cellular process in a 3-D scaffold to primarily chemical modification. It makes the interpretation of *in vitro* analysis results more straightforward.

In this study, we probed the interaction between osteosarcoma TE85 cells and anionic ligands with potential mineral binding capabilities. Cell attachment and proliferation were not adversely affected by the anionic ligands displayed on functionalized slides. Instead, the anionic surfaces promoted the expression of osteogenic marker proteins osteocalcin and alkaline phosphatase, as well as ECM proteins fibronectin and vitronectin under differentiation culture conditions. Microarray analysis confirmed that culturing TE85 over anionic surfaces does not activate apoptotic pathways. Collectively, these results suggest from a biocompatibility standpoint that the mineral-binding anionic ligands examined here may be used in the further development of 3-D artificial bone-like scaffolds. It is worth noting that although osteosarcoma cell lines have been shown to be appropriate models for studying integrin subunit expression, cell adhesion, and the regulation and production of osteocalcin, it is arguable whether they are suitable models for studying proliferation and alkaline phosphatase activities.[34] It remains to be seen how normal human osteoblasts respond to these ligands.

This method can also be extended to other tissue engineering applications *via* linker manipulation and alternative coupling chemistries. A wide range of ECM mimetics (*e.g.* proteins, peptides, oligo- and polysaccharides) intended for artificial tissues can be directly exposed on a 2-D platform and cellular responses to these chemical ligands can be analyzed before the construction of a 3-D scaffold is pursued.

Acknowledgements

The functionalization and characterization of 2-D surfaces, cell culture and protein-based *in vitro* analyses were supported by the National Institute of Health grant No. R01 DE015633-01 under the U.S. Department of Energy Contract No. DE-AC03-76SF00098. The microarray analyses were supported by a Whitaker Leadership Award (funding to CMK) and the Director, Office of Science, Office of Basic Energy Sciences, Division of Materials Sciences and Engineering, of the U.S. Department of Energy under Contract No. DE-AC03-76SF00098.

References

1 S. T. Boyce, *Burns*, 2001, **27**, 523–533.
2 L. Lu, X. Zhu, R. G. Valenzuela, B. L. Currier and M. J. Yaszemski, *Clin. Orthop.*, 2001, **391**, S251–270.
3 T. Shimizu, M. Yamato, A. Kikuchi and T. Okano, *Biomaterials*, 2003, **24**, 2309–2316.
4 S. Yang, K. F. Leong, Z. Du and C. K. Chua, *Tissue Eng.*, 2001, **7**, 679–689.
5 C. R. Lee, A. J. Grodzinsky and M. Spector, *Biomaterials*, 2001, **22**, 3145–3154.
6 Z. Feng, M. Yamato, T. Akutsu, T. Nakamura, T. Okano and M. Umezu, *Artif. Organs*, 2003, **27**, 84–91.
7 C. M. Klapperich and C. R. Bertozzi, *Biomaterials*, 2004, **25**, 5631–5641.
8 K. Webb, V. Hlady and P. A. Tresco, *J. Biomed. Mater. Res.*, 1998, **41**, 422–430.
9 K. E. Healy, *Curr. Opin. Solid State Mater. Sci.*, 1999, **4**, 381–387.
10 R. F. S. Lenza, W. L. Vasconcelos, J. R. Jones and L. L. Hench, *J. Mater. Sci., Mater. Med.*, 2002, **13**, 837–842.
11 R. F. S. Lenza, J. R. Jones, W. L. Vasconcelos and L. L. Hench, *J. Biomed. Mater. Res.*, 2003, **67A**, 121–129.
12 P. F. M. Choong, T. J. Martin and K. W. Ng, *J. Orthop. Res.*, 1993, **11**, 638–647.
13 C. Maniatopoulos, J. Sodek and A. Melcher, *Cell Tissue Res.*, 1988, **254**, 317–330.
14 J. B. Lian and G. S. Stein, *J. Oral Implant.*, 1993, **19**, 95–105.
15 Z. J. Gartner, M. W. Kanan and D. R. Liu, *Angew. Chem., Int. Ed.*, 2002, **41**, 1796–1800.
16 P. Fante, M. S. Kindy, S. Mohaparta, J. Klein, G. Colombo and H. H. Malluche, *Am. J. Physiol.*, 1992, **263**, E1113–E1118.
17 G. N. Bancroft, V. I. Sikavitsas, J. van den Dolder, T. L. Sheffield, C. G. Ambrose, J. A. Jansen and A. G. Mikos, *Proc. Natl. Acad. Sci.USA*, 2002, **99**, 12600–12605.
18 R. A. e. a. Irizarry, *Nucl. Acids Res.*, 2003, **31**, e15.
19 R. A. e. a. Irizarry, *Biostat.*, 2003, **4**, 249–264.
20 Y. H. Hu, S. R. Winn, I. Krajbich and J. O. Hollinger, *J. Biomed. Mater. Res.*, 2003, **64A**, 583–590.
21 W. R. Gombotz and A. S. Hoffman, *Abstr. Pap. Am. Chem. Soc.*, 1987, **193**, 163–PMSE.
22 C. L. Rinsch, X. Chen, V. Panchalingam, C. R. Savage, Y. H. Wang, R. C. Eberhart and R. B. Timmons, *Abstr. Pap. Am. Chem. Soc.*, 1995, **209**, 141-POLY Part 142.
23 D. A. Puleo, R. A. Kissling and M.-S. Sheu, *Biomaterials*, 2002, **23**, 2079–2087.
24 A. George, L. Bannon, B. Sabsay, J. W. Dillon, J. Malone, A. Veis, N. A. Jenkins, D. J. Gillbert and N. G. Copeland, *J. Biol. Chem.*, 1996, **271**, 32869–32873.
25 G. K. Hunter and H. A. Goldberg, *Biochem. J.*, 1994, **302**, 175–179.
26 H. A. Goldberg, K. J. Warner, M. J. Stillman and G. K. Hunter, *Connect Tissue Res.*, 1996, **35**, 439–446.
27 C. E. Tye, K. R. Rattray, K. J. Warner, J. A. R. Gordon, J. Sodek, G. K. Hunter and H. A. Goldberg, *J. Biol. Chem.*, 2003, **278**, 7949–7955.
28 A. Veis and A. Perry, *Biochemistry*, 1967, **6**, 2409–2416.
29 R. M. McAllister, M. B. Gardner, A. E. Greene, C. Bradt, W. W. Nichols and B. H. Landing, *Cancer*, 1971, **27**, 397–402.
30 J. S. Rhim, H. Y. Cho and R. J. Huebner, *Int. J. Cancer*, 1975, **15**, 23–29.
31 A. Purohit, A. M. Flanagan and M. J. Reed, *Endocrinology*, 1992, **131**, 2027–2029.
32 E. Kyeyunenyombi, K. H. W. Lau, D. J. Baylink and D. D. Strong, *Clin. Res.*, 1990, **38**, A122–A122.
33 K. H. W. Lau, A. Yoo and S. P. Wang, *Mol. Cell. Biochem.*, 1991, **105**, 93–105.
34 J. Clover and M. Gowen, *Bone*, 1994, **15**, 585–591.
35 J. Takada, T. Chevalley, D. J. Baylink and K. H. W. Lau, *Calcif. Tissue Int.*, 1996, **58**, 355–361.
36 J. W. Gunnet, K. Granger, E. Cryan and K. T. Demarest, *J. Endocrinol.*, 1999, **163**, 139–147.
37 M. Amoui, D. J. Baylink, J. B. Tillman and K. H. W. Lau, *J. Biol. Chem.*, 2003, **278**, 44273–44280.
38 H. Mitsuyama, F. Kambe, R. Murakami, X. Cao, N. Ishiguro and H. Seo, *J. Bone Miner. Res.*, 2004, **19**, 671–679.
39 J. B. Lian and G. S. Stein, *Crit. Rev. Oral Biol. Med.*, 1992, **3**, 269–305.
40 P. V. Hauschka, J. B. Lian, D. E. C. Cole and C. M. Gundberg, *Physiol. Rev.*, 1989, **69**, 990–1047.
41 R. Edgar, M. Domrachev and A. E. Lash, *Nucl. Acids Res.*, 2002, **30**, 207–210.